Bioorganic & Medicinal Chemistry 17 (2009) 2154–2161

Contents lists available at ScienceDirect

Bioorganic & Medicinal Chemistry

journal homepage: www.elsevier.com/locate/bmc

Probing natural product biosynthetic pathways using Fourier transform ion cyclotron resonance mass spectrometry

Xidong Feng *, Anokha S. Ratnayake, Romila D. Charan, Jeffrey E. Janso, Valerie S. Bernan, Gerhard Schlingmann, Haiyin He, Mark Tischler, Frank E. Koehn, Guy T. Carter *

Chemical and Screening Sciences, Wyeth Research, 401 N. Middletown Road, Pearl River, NY 10965, USA

ARTICLE INFO

Article history:
Received 20 June 2008
Revised 26 September 2008
Accepted 31 October 2008
Available online 5 November 2008

Keywords:
FTMS
Natural products biosynthesis
Stable-isotope labeling dioxapyrrolomycin
Diazepinomicin

ABSTRACT

Two natural products, diazepinomicin (**1**) and dioxapyrrolomycin (**2**), containing stable isotopic labels of ^{15}N or deuterium, were used to demonstrate the utility of Fourier transform ion cyclotron resonance mass spectrometry for probing natural product biosynthetic pathways. The isotopic fine structures of significant ions were resolved and subsequently assigned elemental compositions on the basis of highly accurate mass measurements. In most instances the mass measurement accuracy is less than one part per million (ppm), which typically makes the identification of stable-isotope labeling unambiguous. In the case of the mono-^{15}N-labeled diazepinomicin (**1**) derived from labeled tryptophan, tandem mass spectrometry located this ^{15}N label at the non-amide nitrogen. Through the use of exceptionally high mass resolving power of over 125,000, the isotopic fine structure of the molecular ion cluster of **1** was revealed. Separation of the $^{15}N_2$ peak from the isobaric $^{13}C^{15}N$ peak, both having similar abundances, demonstrated the presence of a minor amount of doubly ^{15}N-labeled diazepinomicin (**1**). Tandem mass spectrometry amplified this isotopic fine structure (Δm = 6.32 mDa) from mDa to 1 Da scale thereby allowing more detailed scrutiny of labeling content and location. Tandem mass spectrometry was also used to assign the location of deuterium labeling in two deuterium-labeled diazepinomicin (**1**) samples. In one case three deuterium atoms were incorporated into the dibenzodiazepine core; while in the other a mono-D label was mainly incorporated into the farnesyl side chain. The specificity of ^{15}N-labeling in dioxapyrrolomycin (**2**) and the proportion of the ^{15}N-label contained in the nitro group were determined from the measurement of the relative abundance of the $^{14}NO_2^{1-}$ and $^{15}NO_2^{1-}$ fragment ions.

1. Introduction

Natural products (NP) and their derivatives, having been fine tuned by nature through evolutionary selection, have been the single most important source of therapeutic agents owing to their unique chemical structures and biological activities.[1–3] Detailed understanding of NP biosynthetic pathways is not only of fundamental scientific interest but also of great practical significance in pharmaceutical research since the knowledge of the pathways can be used to generate structural modifications through genetic engineering.[4,5] Incorporation experiments with stable isotopically labeled precursors, for example, ^{15}N-, and deuterium, is a common and effective way to probe biosynthetic pathways. The incorporation patterns observed through labeling experiments is useful in unraveling biosynthetic mechanisms.

Location of the atomic labels and accurate measurement of the isotopic labeling content are critical in understanding biosynthetic mechanisms. Mass spectrometry offers the advantage of high sensitivity, which is often required to evaluate the products of small-scale incorporation experiments. Fourier transform ion cyclotron resonance mass spectrometry (FTICR-MS or FTMS)[6,7] with ultra-high resolution and accurate mass measurement (AMM) capabilities is particularly powerful in studying stable-isotope-labeled compounds. Mass resolving power (resolution) was defined as the ratio of the ion mass over the mass spectral peak full width at half maximum peak height (FWHM). Since the mass resolving power is proportional to the magnetic field strength, high-field superconducting magnets were generally equipped with FTMS instruments to achieve ultra-high mass resolving power while minimizing the coalescence effect of the isotopic fine structure peaks.[8] The exceptionally high mass resolving power routinely achieved in FTMS enables the deconvolution of isotopic fine structures (i.e., combination of isobaric species with a difference in mass of only a few mDa) within a nominal unit mass and thereby reveal the presence and abundance of the stable isotopic label such as ^{15}N and D.[9] Measurement of the accurate mass values of the resolved ions with 1-ppm accuracy leads to the unambiguous assignment of elemental composition for totally unknown molecular or fragment

* Corresponding authors. Tel.: +1 845 602 3955; fax: +1 845 602 2969 (X.F.); tel.: +1 845 602 3594; fax: +1 845 602 6005 (G.T.C.).
E-mail addresses: fengx@wyeth.com (X. Feng), carterg@wyeth.com (G.T. Carter).

0968-0896/$ - see front matter © 2008 Elsevier Ltd. All rights reserved.
doi:10.1016/j.bmc.2008.10.073

ions (up to ~400 Da).[10] Tandem mass spectrometry (FTMS/MS or FTMS^n) can be performed on an isolated single (nominal) isotopic peak using either sustained off-resonance irradiation (SORI) coupled with collision induced dissociation (CID)[11] or infrared multi-photon dissociation (IRMPD).[12] The resulting fragment ions can also be measured with ultra-high resolution and mass accuracy to determine elemental compositions and fragmentation pathways, thereby facilitating the location of labeled atoms. Stable isotopic enrichments often complicates the natural isotopic distribution, so that some labeling information might be masked in a single (nominal) isotopic peak consisting of naturally occurring and labeled isobaric peaks with a difference in mass of only a few mDa, for example, the $^{15}N_2$-labeled peak and the isobaric $^{13}C^{15}N$ peak with Δm = 6.32 mDa. In certain cases, the FTMS/MS can amplify this isotopic fine structure from mDa to the one Da scale allowing detailed scrutiny of the labeling content and distribution.

Two novel natural products, diazepinomicin (**1**)[13,14] and dioxapyrrolomycin (**2**)[15,16] (Fig. 1) are used in this report as examples to illustrate the utility of FTMS in the study of biosynthetic pathways through stable-isotope incorporation experiments. Diazepinomicin (**1**), a dibenzodiazepine alkaloid was isolated from the fermentation broth of marine-derived *Micromonospora* sp. strains. The dibenzodiazepine core structure in **1** is exceptionally rare among natural products; therefore the investigation of the precursors of the diazepine ring system is of fundamental interest. In order to probe the biosynthetic origin of the carbon skeleton and the nitrogen atoms in the core structure of **1**, feeding experiments with a series of ^{15}N and deuterium isotope-labeled precursors were carried out and the resulting isotopically labeled products were analyzed using FTMS and FTMS/MS.

Dioxapyrrolomycin (**2**), a poly-halogenated, nitropyrrole-containing antibiotic was isolated from a terrestrial actinomycete culture LL-F42248. A remarkable feature of this producing organism is its ability to carry out direct biochemical nitration of the pyrrole moiety.[17] The mechanism of nitration in pyrrolomycin antibiotics has been a topic of interest for many years, and consequently, several research groups have provided valuable insights into possible nitration mechanisms.[18–20] Despite these efforts, the biochemical details of the origin of the nitro group in **2** remain ambiguous, therefore incorporation experiments with a series of ^{15}N-labeled precursors (arginine and proline) have been carried out in our group to better understand the biosynthetic mechanism of dioxapyrrolomycin nitration. Owing to its heavy chlorine content, dioxapyrrolomycin (**2**) has a complex isotopic distribution, which is further compounded by the incorporation of the ^{15}N labels. Fortunately, the nitro group can be readily cleaved and subsequently measured by FTMS/MS.

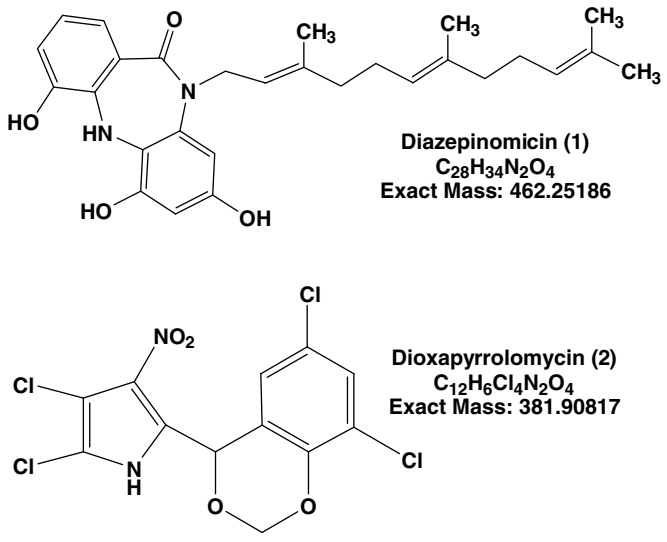

Figure 1. Molecular structures of diazepinomicin (**1**) and dioxapyrrolomycin (**2**).

The complete study of the biosynthetic pathways for diazepinomicin (**1**) and dioxapyrrolomycin (**2**) will be published elsewhere.[21] In this report, we will focus primarily on the results from FTMS measurements that demonstrate its utility in probing biosynthetic processes.

2. Results and discussion

2.1. Diazepinomicin (1)

Diazepinomicin (**1**), a novel bioactive alkaloid, was isolated from the culture broth of a marine actinomycete belonging to the genus *Micromonospora*. The same compound was also discovered essentially simultaneously by Bachmann et al. and was advanced into clinical development as an anticancer agent.[14] FTMS analysis of products derived from ^{15}N-labeled L-tryptophan, deuterium-labeled L-tryptophan (indole-D_5), and D_4-L-tyrosine (phenyl-D_4) was employed to probe the biosynthesis of **1**.

2.1.1. ^{15}N-labeled diazepinomicin

When $^{15}N_2$-labeled tryptophan was supplemented in the growth medium, mono-^{15}N and $^{15}N_2$-labeled diazepinomicin (**1**) were produced as shown by nanoelectrospray FTMS analysis (Fig. 2). In this experiment the singly labeled species was the major product as evidenced by the $[M+Na]^{1+}$ and $[M+H]^{1+}$ molecular ions. A smaller proportion of doubly ^{15}N-labeled product is also observed (ca. 17%), as well as approximately 7% of unlabeled material. In the mass range two nominal mass units higher than the unlabeled product, the $^{15}N_2$ ions are resolved from the isobaric $^{13}C^{15}N$ species, for both the $[M+H]^{1+}$ and the $[M+Na]^{1+}$ molecular ions. The separation of these ions illustrates the tremendous resolving power (125,000 FWHM, for the *m*/*z* 486 peak) of FTMS. Without sufficient resolution (below 74,000), the doublet peaks would have collapsed into one and could be mistakenly interpreted as the naturally occurring ^{13}C isotope of the mono-^{15}N-labeled **1** only, and the $^{15}N_2$-labeled species would be masked.

Since there are two nitrogen atoms in diazepinomicin, the distribution of label in the mono-^{15}N-labeled species was investigated by FTMS/MS experiments. SORI-CID of the isolated ion at *m*/*z* 464 was employed to create fragment ions. In our previous report,[13] three major fragment ions at *m*/*z* 271, 259, and 243, were detected using FTMS/MS for the isolated monoisotopic peak at *m*/*z* 463 $[M+H]^{1+}$ for unlabeled **1** as shown in Figure 3A. The fragmentation pathways are shown in the inset of Figure 3A. In the SORI-CID mass spectrum of the isotopic peak at *m*/*z* 464 for $[M+H]^{1+}$ of the mono-^{15}N-labeled species, these fragment ions all appeared at 1 Da higher relative to their unlabeled counterpart peaks, as shown in Figure 3B. The fragment ion at *m*/*z* 244, resulting from the excision of the farnesylamine portion of the amide moiety, still retains the ^{15}N label and therefore it is the non-amide nitrogen that was labeled. A much less abundant peak at *m*/*z* 243.05287 ($C_{13}H_9NO_4^{1+}$, pred, 243.05261) was also detected, corresponding to the same sub-structure of *m*/*z* 244 without ^{15}N label, but it could be accounted as the dissociation of the ^{13}C isotope of the unlabeled **1** (~7% as shown in Figure 2), consequently the non-amide nitrogen in the mono-^{15}N-labeled **1** carried virtually all the mono-^{15}N label.

The high specific incorporation of the ^{15}N label into the non-amide nitrogen is interpreted as an indication of the incorporation of an intermediate directly derived from tryptophan, rather than a general enrichment of the ^{15}N pool through catabolism. It is postulated that the tryptophan is first degraded into 3-hydroxyanthrani-

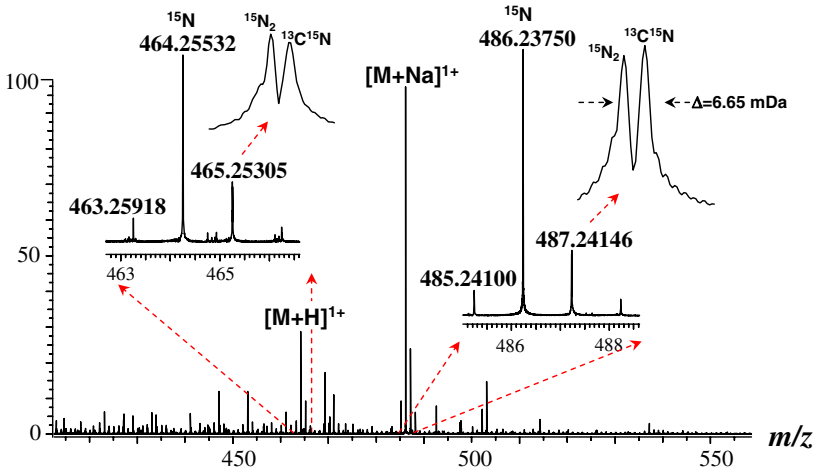

Figure 2. Positive mode nanoelectrospray FTMS mass spectrum of ^{15}N-labeled diazepinomicin (**1**) with $^{15}N_2$-labeled tryptophan feeding.

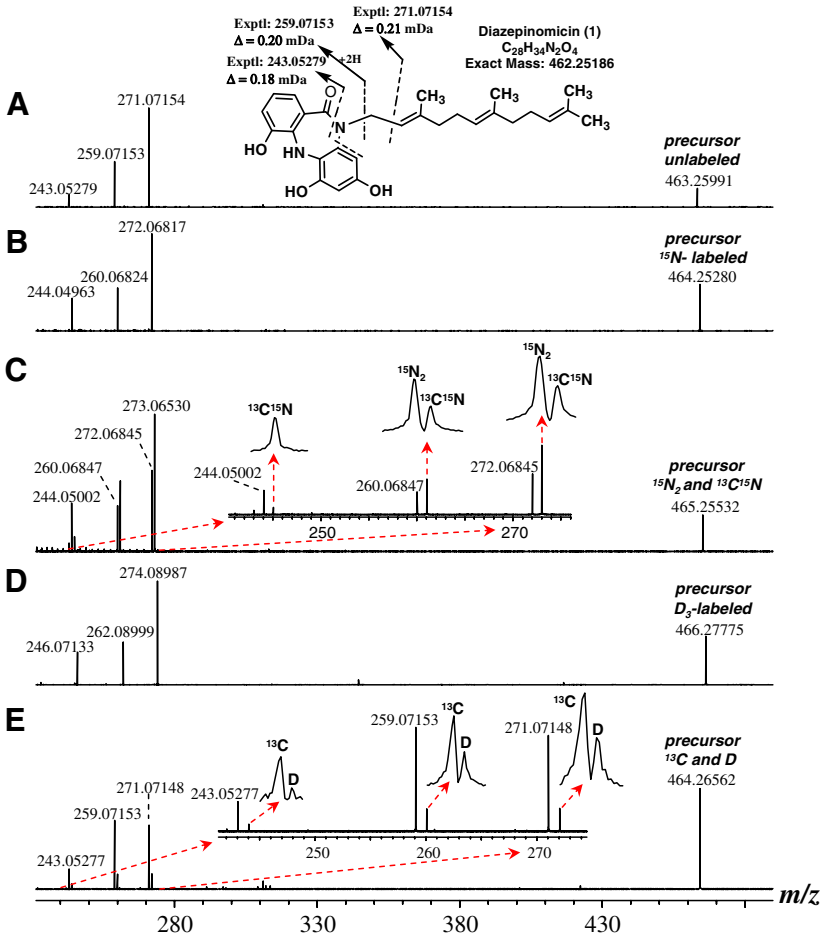

Figure 3. Positive mode nanoelectrospray FTMS/MS (IRMPD for **C** and SORI-CID for the rest) spectrum of the isolated $[M+H]^{1+}$ molecular ion for (A) unlabeled **1** at *m/z* 463 and the proposed fragmentation pathways (inset), (B) mono-^{15}N-labeled **1** at *m/z* 464 from ^{15}N-labeled tryptophan feeding, (C) $^{15}N_2$-labeled **1** at *m/z* 465 from ^{15}N-labeled tryptophan feeding, (D) D_3-labeled **1** at *m/z* 466 from tryptophan-D_5 (indole-D_5) feeding, (E) mono-D-labeled **1** at *m/z* 464 from D_4-L-tyrosine (phenyl-D_4) feeding.

lic acid which is then incorporated through condensation with the precursor of the other phenyl ring. In this process the ring nitrogen of tryptophan is incorporated into the diazepine ring as the non-amide nitrogen.

There is solid evidence to support the assignment of the revealed $^{15}N_2$ isobaric peak as a real species rather than an artifact. First, the same isotopic fine structure was detected for both the $[M+H]^{1+}$ and the $[M+Na]^{1+}$ molecular ions. The measured mass differences between the two isobaric peaks were 6.34 mDa and 6.65 mDa for the $[M+H]^{1+}$ and $[M+Na]^{1+}$ molecular ions, respectively, which agreed very well with the predicted $\Delta m = 6.32$ mDa between $^{15}N_2$ and $^{13}C^{15}N$ isobaric peaks. Secondly, the measured

mass differences between the mono-^{15}N peak and the $^{15}N_2$ peak were 0.99773 Da and 0.99731 Da for the $[M+H]^{1+}$ and $[M+Na]^{1+}$ molecular ions, respectively, which agreed very well with the predicted value of 0.99703 Da. Such small mass differences can be measured very accurately and reliably and they are extremely specific for peak assignments. Finally the high mass accuracy for every resolved isotopic peak adds confidence to the assignments.

The fragmentation behavior of the $^{15}N_2$-labeled species was studied by isolating the *m*/*z* 465 peak using a correlated harmonic excitation fields (CHEF) and then dissociated by IRMPD (Fig. 3C). The same three major fragment ions at *m*/*z* 272, 260, and 244 detected in the SORI-CID mass spectrum of the *m*/*z* 464 (mono-^{15}N-labeled **1**) ion were detected again. In this case additional ions of nominal mass +1 Da emerged for each of the three sub-structures as shown in the expansion of Figure 3C. Two of these are narrowly resolved doublet peaks at *m*/*z* 273 and *m*/*z* 261. The fragment ions at *m*/*z* 272, 260, and 244 are the result of the dissociation of the $^{13}C^{15}N$ isotopic species contained in the precursor ion at *m*/*z* 465. This $^{13}C^{15}N$ species is also responsible for the generation of the $^{13}C^{15}N$ component of the doublet peaks at *m*/*z* 273 and *m*/*z* 261. The remaining ion for each of the two doublet peaks at *m*/*z* 273 and *m*/*z* 261 was assigned an elemental composition containing two ^{15}N atoms, as the result of the dissociation of the $^{15}N_2$ species contained in the precursor ion at *m*/*z* 465. The results obtained by the FTMS/MS experiment amplified the isotopic fine structure of the precursor ions from a few mDa scale to 1 Da scale, making the assignment of $^{15}N_2$-labeling unequivocal.

The relatively low abundance of the ^{15}N label found in the amide nitrogen suggests that this incorporation is less directly linked to intact tryptophan. It may be that the nitrogen has been recycled into the general metabolic pool of the organism through catabolic pathways.

2.1.2. Deuterium-labeled diazepinomicin

When L-tryptophan (indole-D_5) precursor was supplemented in the fermentation medium, D_3-labeled **1** was the most abundant product as evidenced by the detection of the D_3 versions of both the $[M+H]^{1+}$ and $[M+Na]^{1+}$ molecular ions in the positive mode nanoelectrospray FTMS (Table 1 and Supplementary Materials Fig. S1). Concurrently, the D_2-labeled molecular ions were also detected, but at much lower abundance. The measured relative abundances for D_2-labeled and unlabeled peaks ($[M+Na]^{1+}$) were 4% and 10%, respectively, taking the abundance of the D_3-labeled peak as 100%.

To locate the sites of deuterium labeling, the FTMS SORI-CID experiment was conducted on the $[M+H]^{1+}$ molecular ion at *m*/*z* 466 for the D_3-labeled species. The resulting mass spectrum (Fig. 3D) is very similar to that detected for the $[M+H]^{1+}$ ion at *m*/*z* 463 of the unlabeled **1** (Fig. 3A), except that the three major fragment ions at *m*/*z* 246, 262, and 274 were all shifted three Da ($D_3 - H_3 = 3.01883$ Da; exptl, 3.01844 Da) higher relative to their counterpart peaks detected for unlabeled **1**. Therefore it was concluded that the dibenzodiazepine core structure carries all three deuterium atoms. This finding is consistent with the previous ^{15}N-labeling result with tryptophan showing catabolism to 3-hydroxyanthranilic acid occurs prior to incorporation. Although it is anticipated that the three deuterium atoms are on the phenyl ring derived from tryptophan, there is no specific fragment ion in the MS/MS data that directly supports this hypothesis. The precise location of these atoms was determined on the phenyl ring in an NMR experiment.[21]

When D_4-L-tyrosine (phenyl-D_4) was incorporated in the fermentation medium, the resultant deuterium enriched product had a very different labeling pattern as determined by FTMS (Supplementary Materials Table S1). Under ultra-high resolution conditions (300,000 FWHM) the isotopic fine structures were completely resolved for the isobaric peaks at *m*/*z* 462, *m*/*z* 463, and *m*/*z* 464 of the $[M-H]^{1-}$ molecular ion (Fig. 4). Specifically, the mono-deuterated peak was separated from the naturally occurring ^{13}C isotopic peak for the *m*/*z* 462 peak, demonstrating the presence of the mono-D-labeled species with relative abundance of 54% to the unlabeled species at *m*/*z* 461. The D_2-labeled peak was separated from the naturally occurring $^{13}C_2$ isotopic peak and the ^{13}CD isotopic peak of the mono-D-labeled species for the *m*/*z* 463 peak, with relative abundance of 24%, and the D_3-labeled peak was separated from the $^{13}CD_2$ isotopic peak of the D_2-labeled species for the *m*/*z* 464 peak, with relative abundance of 8% to the unlabeled species at *m*/*z* 461. The proportion of mono-deuterated **1** could be estimated as 54%/(100% + 54% + 24% + 8%) = 29%. Likewise, the proportions of D_2- and D_3-labeled **1** were estimated to be 13% and 4%, respectively. Essentially the same isotopic fine structures were detected for both the $[M+H]^{1+}$ (data not shown) and the $[M+Na]^{1+}$ (Supplementary Materials Table S1) molecular ions in the positive mode nanoelectrospray mass spectrum. The molecular ion mass spectrum in the positive mode was not shown here owning to its relatively poor quality compared with the negative mode mass spectrum. In comparison to the results obtained in the tryptophan (indole-D_5) labeling experiments the incorporation rate was substantially lower, with the unlabeled product predominating. The ultra-high mass resolving power is essential to completely resolve the isobaric peaks and therefore allow for detailed interpretation of the stable isotopic incorporation. It would be difficult to quantify any enrichment by low resolution mass measurements in this case.

The protonated $[M+H]^{1+}$ molecular ion, instead of the deprotonated $[M-H]^{1-}$, was selected for the FTMS/MS study to locate the sites of deuterium labeling for the mono-deuterated species, as the $[M+H]^{1+}$ molecular ion fragmentation pathways have been fully characterized and used earlier to locate the labeling sites. The *m*/*z* 464 peak from the $[M+H]^{1+}$ molecular ion, containing two major isobaric ions ^{13}C and D, was isolated using CHEF and then dissociated by SORI-CID (Fig. 3E). The three major fragment ions at *m*/*z* 271, 259, and 243 are essentially the same as those observed in the SORI-CID mass spectrum of the $[M+H]^{1+}$ molecular ion at *m*/*z* 463 for the unlabeled compound (Fig. 3A), indicating

Table 1
Accurate mass measurement for the D-labeled diazepinomicin with tryptophan-D_5 feeding by nanoelectrospray FTMS.

Molecular ion	Elemental	Exptl	Pred	Error[a] (mDa)	Structure assignment	Rel. abun. (%)	Portion[b] (%)
$[M+H]^{1+}$	$C_{28}H_{35}N_2O_4^{1+}$	463.26013	463.25914	0.99	Monoisotope	2	8
	$C_{28}H_{33}D_2N_2O_4^{1+}$	465.27069	465.27169	−1	D_2 labeling	2	8
	$C_{28}H_{32}D_3N_2O_4^{1+}$	466.27855	466.27797	0.58	D_3 labeling	20	84
$[M+Na]^{1+}$	$C_{28}H_{34}N_2O_4Na^{1+}$	485.24198	485.24108	0.9	Monoisotope	10	8
	$C_{28}H_{32}D_2N_2O_4Na^{1+}$	487.25402	487.25363	0.39	D_2 labeling	4	4
	$C_{28}H_{31}D_3N_2O_4Na^{1+}$	488.25934	488.25991	−0.57	D_3 labeling	100	88

[a] Errors (mDa) were calculated as experimental value − predicted value.
[b] See Section 4.3 for calculation details.

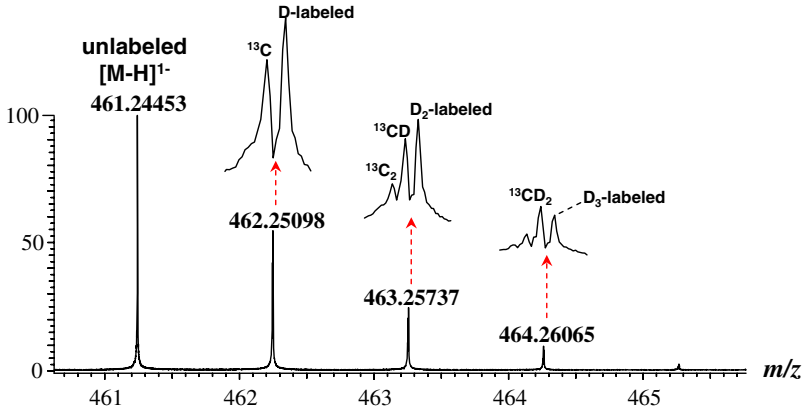

Figure 4. Mass scale-expanded segment of the negative mode nanoelectrospray FTMS mass spectrum for deuterium-labeled diazepinomicin with D_4-L-tyrosine (phenyl-D_4) feeding. The resolved isotopic fine structures are plotted above, showing the D-, D_2-, and D_3-labeled peaks.

clearly that the dibenzodiazepine core was not the primary site of deuterium labeling. The deuterium-containing components of these key fragment ions are resolved from the ^{13}C species in the expansion shown in Figure 3E. The low abundance of the deuterium-containing ions is simply an indication that the deuterium-labeled tyrosine was thoroughly catabolized by the organism. Presumably additional deuterium atoms are distributed in the farnesyl moiety through incorporation of the catabolic products of tyrosine.

2.2. Dioxapyrrolomycin (2)

In order to gain additional insight into the biosynthetic origin of the nitro group in dioxapyrrolomycin (**2**), four feeding experiments incorporating different combinations of ^{15}N stable-isotope-labeled precursors were carried out. Accordingly, cultures of the producing organism were supplemented with (**A**) L-[^{15}N]-proline and L-arginine, (**B**) L-[$^{15}N_2$]-guanidino-arginine and L-proline, (**C**) L-[U$^{15}N_4$]-arginine and L-proline, and (**D**) L-[^{15}N]-proline. The resulting ^{15}N-labeled dioxapyrrolomycin samples were investigated using FTMS and FTMS/MS. The structures and the fragmentation pathways of the $[M-H]^{1-}$ molecular ions of dioxapyrrolomycin and its analogues have been studied in great detail.[16,18] Facile loss of formaldehyde from the methylenedioxy group of **2** was readily induced by CID or in-source fragmentation (Fig. 5). The $-NO_2$ group of **2** is readily cleaved and subsequently detected in negative mode electrospray (ESI) FTMS SORI-CID or IRMPD mass spectrometry. The measured isotopic distribution of nitrogen in the NO_2^{1-} fragment ion has been used to determine the extent and specificity of incorporation of the various nitrogenous precursors.

Figure 5A–D shows the negative mode ESI FTMS spectra of ^{15}N-labeled **2** obtained under the growth conditions **A**–**D**, respectively. Isotopic distributions with increasing complexity were observed, owing to the four chlorine substituents and further complicated by the incorporation of the ^{15}N-labels. Fortunately, the isotopic fine structure is readily resolved with the high resolving power of FTMS and the isotopic composition of the peaks can be reliably assigned. Mono-^{15}N-labeled product was detected under conditions **A** and **B**, together with the unlabeled species. The proportion of the mono-^{15}N-labeled species was estimated (Section 4.4) as ~54% with the remaining proportion (~46%) unlabeled in case **A**, and 50% was mono-^{15}N labeled for case **B** (Supplementary Materials Table S2).

In cases **C** and **D** doubly ^{15}N-labeled dioxapyrrolomycin (**2**) was produced together with the mono-^{15}N-labeled and unlabeled **2**, as shown in Figure 5C and D, respectively. The proportions of unlabeled, mono-^{15}N labeled, and $^{15}N_2$-labeled products are estimated as ~14%, ~53%, and ~33%, respectively, for case **C**. In case **D**, unlabeled **2** was negligible, while $^{15}N_2$-labeled was the major species (~77%) and the mono-^{15}N-labeled **2** was ~22%. (Supplementary Materials Table S2).

The resolution of the isotopic fine structure is critical in case **C** to separate the isobaric peaks for clear confirmation of the $^{15}N_2$ enrichment, which would be likely masked under low resolution mass measurements. Two major isobaric peaks were resolved for the *m*/*z* 383 peak with achieved resolving power of over 257,000 as shown in the inset of Figure 5C (peak marked with *), one with *m*/*z* 382.89776, corresponding to the heavier isotope (^{37}Cl) of the unlabeled **2** ($C_{12}H_5Cl_3{}^{37}ClN_2O_4{}^{1-}$, pred. 382.89794, $\Delta = -0.18$ mDa), and the other with *m*/*z* 382.89460, corresponding to the $[M-H]^{1-}$ molecular ion of $^{15}N_2$-labeled **2** (Supplementary Materials Table S2). A third isobaric peak at *m*/*z* 383 was also resolved, corresponding to the heavier isotope (^{13}C) of the mono-^{15}N-labeled **2** ($C_{11}{}^{13}CH_5Cl_4N{}^{15}NO_4{}^{1-}$, exptl. 382.90134, pred. 382.90128, $\Delta = 0.06$ mDa), but with much lower abundance.

The relative distribution of ^{15}N between the pyrrole and nitro groups was evaluated by examination of the NO_2^{1-} ion formed in the FTMS/MS experiment. The negative mode ESI FTMS SORI-CID experiments were conducted on the isolated *m*/*z* 382 peak (mono-^{15}N) as shown in Figure 5A1–D1 with expanded view in the inset of each spectrum showing the isotopic distribution of the NO_2^{1-} fragment ion. The unlabeled ($^{14}NO_2{}^{1-}$) fragment ion was the major species (Supplementary Materials Table S3) in cases **A** and **D**, indicting that the nitro group was only marginally labeled and consequently the ^{15}N label was predominantly incorporated into the pyrrole nitrogen. The portions of mono-^{15}N-labeled dioxypyrrolomycin (**2**) with the nitro group ^{15}N-labeled were estimated (Section 4.5) to be only 7% and 12% for cases **A** and **D**, respectively (Table 2). In case **A** this is not unexpected since it is known that proline is a direct precursor of the pyrrole portion of **2**. The low abundance of ^{15}N label in the $-NO_2$ group for the mono-^{15}N-labeled species in case **D** is surprising since the medium contained only ^{15}N-proline as the sole nitrogen source. This finding has led to the hypothesis that the organism is capable of fixing nitrogen, as no other source of isotopic dilution was possible in the experiment. Additional experiments are ongoing to investigate this phenomenon.

In contrast, the $^{15}NO_2{}^{1-}$ fragment ion is highly abundant in cases **B** and **C**, (Fig. 5B1 and C1, Supplementary Materials Table S3) showing that a large proportion of the mono- ^{15}N label is in the nitro group. The proportions of mono-^{15}N-labeled **2** bearing a

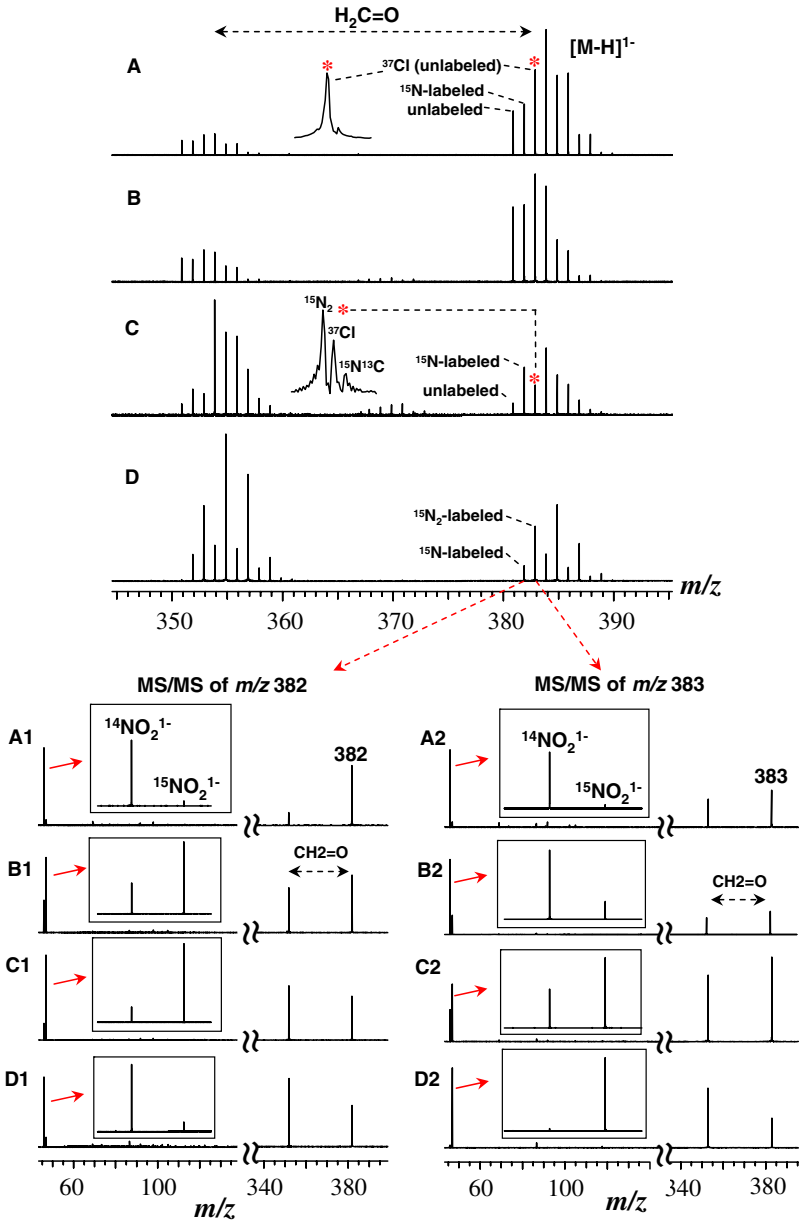

Figure 5. Negative mode ESI FTMS and FTMS/MS mass spectrum of the $[M-H]^{1-}$ molecular ion for ^{15}N-labeled dioxapyrrolomycin (**2**) isolated from feeding experiments with (A) L-[^{15}N]-proline and L-[^{14}N]-arginine, (B) L-[^{15}N]-guanidino-arginine and L-[^{14}N]-proline, (C) L-[$U^{15}N_4$]-arginine and L-[^{14}N]-proline, and (D) L-[^{15}N]-proline. Insets in (A) and (C) show the expanded view of the isotopic peaks labeled with asterisk.

Table 2
Portions of mono-^{15}N-labeled dioxypyrrolomycin (**2**) with the nitro group ^{15}N-labeled or unlabeled.

	Case **A**	Case **B**	Case **C**	Case **D**
	L-[^{15}N]-Pro, L-Arg	L-[$^{15}N_2$]-i-Arg, L-Pro	L-[$U^{15}N_4$]-Arg, L-Pro	L-[^{15}N]-Pro
Portion with $^{15}NO_2$[a] (%)	7	77	85	12
Portion with $^{14}NO_2$ (%)	93	23	15	88

[a] See Section 4.5 for calculation details.

^{15}N-labeled nitro group were estimated to be 78% and 86% for cases **B** and **C** (Table 2), respectively, after correction for the interference of the ^{13}C isotopic ion of the unlabeled **2** to the $^{14}NO_2{}^{1-}$ fragment ion (Section 4.5). This rate of incorporation presumably reflects the availability of the nitrogen atoms derived from arginine to feed into the nitration pathway.

3. Conclusion

FTMS with its exceptionally high resolving power is a powerful tool that can be used to reveal the isotopic fine structure for reliable interpretation of the chemistry of biosynthetic processes. Highly accurate mass measurement capability makes the assignment of elemental compositions of the ions unequivocal. FTMS/MS enables the isolation of labeled fragment ions that aid in the identification of specifically labeled atoms as well as providing confirmation of the extent of label incorporation. Ultimately, the

integrated use of high mass accuracy and ultra-high resolution routinely achieved in FTMS and FTMS^n experiments provides a combination of tools that greatly facilitates the detection of stable-isotope labels on small quantities of material.

4. Experimental

4.1. FTMS experiments

High resolution mass spectra were obtained using a Bruker Daltonics (Billerica, MA) APEX II FTICR mass spectrometer equipped with an actively shielded 9.4 T superconducting magnet (Magnex Scientific Ltd, UK), an external Bruker Apollo ESI source, and a Synrad 50 W CO_2 CW laser. Its instrumentation details and application capabilities have been published previously,[22] and in a recent review[7] the FTMS application in natural products discovery efforts based primarily on this instrument has been highlighted. Sustained off-resonance irradiation (SORI) coupled with collision induced dissociation (CID) or infrared multi-photon dissociation (IRMPD) was used to fragment the precursor ion to determine the location of labeled atoms in diazepinomicin (**1**) and dioxapyrrolomycin (**2**). Nanoelectrospray, with its low flow rate and good sensitivity, was utilized to maintain longer period ion signal for detailed experimental study while consuming very limited quantities of natural product samples. About 5 μl sample was loaded into nanoelectrospray tip (New Objective, Woburn, MA) and a high voltage about 1000 V was applied between the nanoelectrospray tip and the capillary. Bruker Xmass software (Versions 5 and 6) was used for data acquisition and analysis, including the calculations for predicted masses with corrections for the mass of the electrons responsible for the charge state of the ion. Mass spectra were calibrated internally or externally using Agilent ES tuning mix (G2421A). The reported errors (Δ) are the differences between the experimental and predicted values expressed in mDa.

4.2. Calculations of the enrichment for ^{15}N-labeled diazepinomicin (1)

The percentage of $^{15}N_2$-labeled diazepinomicin (**1**) could be calculated as follows: $[A_2 - 0.0037 * (A_1 - 0.0074 * A_0)] * 100/[A_0 + A_1 - 0.0074 * A_0 + A_2 - 0.0037 * (A_1 - 0.0074 * A_0)]$, where A_0, A_1, and A_2 are the measured relative abundances for the monoisotopic, ^{15}N-, and $^{15}N_2$-peaks for diazepinomicin (**1**), respectively. Likewise, the percentage of mono-^{15}N-labeled **1** could be calculated using $(A_1 - 0.0074 * A_0) * 100/[A_0 + A_1 - 0.0074 * A_0 + A_2 - 0.0037 * (A_1 - 0.0074 * A_0)]$. The coefficient 0.0074 is the calculated ratios of the peak heights for the naturally occurring ^{15}N isotopic peak over the monoisotopic peak of unlabeled **1**, using Bruker Xmass software (version 5.02). Similarly, 0.0037 is the calculated ratios of the peak heights for the naturally occurring ^{15}N isotopic peak over the first peak of the mono-^{15}N-labeled **1**. The extra terms with coefficients 0.0074 and 0.0037 were considered since the naturally occurring ^{15}N isotopic peaks of the unlabeled and mono-^{15}N-labeled **2** could be resolved with the routinely achieved resolving power over 100,000 (FWHM), however, in practice these terms are very small and thus can be omitted. For the ^{15}N-labeled diazepinomicin (**1**) sample reported in Section 2.1.1, the relative abundances of unlabeled, mono-^{15}N labeled, and $^{15}N_2$-labeled **1** for the sodium adduct ion ($[M+Na]^{1+}$) are 10% (A_0), 100% (A_1), and 23% (A_2), respectively, taking the abundance of the ^{15}N peak as 100% for simplicity. The proportions of **1** with $^{15}N_2$ and mono-^{15}N labels were then calculated as 17% and 76%, respectively, using the formulas given above, and the remaining proportion of 7% was unlabeled **1**.

4.3. Calculations of the deuterium enrichment in diazepinomicin (1) derived from L-tryptophan (indole-D_5) feeding

The measured relative abundances for D_2-labeled and unlabeled diazepinomicin (**1**) ($[M+Na]^{1+}$) were 4% and 10%, respectively, taking the abundance of the D_3-labeled peak as 100% (Table 1 and Supplementary Materials Fig. S1). Therefore the proportion of D_3-labeled **1** could be calculated approximately as 100%/(10% + 4% + 100%) = 88%, the proportion of D_2-labeled **1** as 4%/(10% + 4% + 100%) = 4%, and the remaining ~8% for the unlabeled species.

4.4. Calculations of the enrichment for ^{15}N-labeled dioxapyrrolomycin (2)

In the same way to calculate the incorporation extends for ^{15}N-labeled diazepinomicin (**1**), the percentage of $^{15}N_2$-labeled dioxapyrrolomycin (**2**) could be calculated as follows: $[A_2 - 0.0037 * (A_1 - 0.0074 * A_0)] * 100/[A_0 + A_1 - 0.0074 * A_0 + A_2 - 0.0037 * (A_1 - 0.0074 * A_0)]$, where A_0, A_1, and A_2 are the measured relative abundances for the monoisotopic, ^{15}N-, and $^{15}N_2$-peaks for dioxapyrrolomycin (**2**), respectively. Likewise, the percentage of mono-^{15}N-labeled **2** could be calculated using $(A_1 - 0.0074 * A_0) * 100/[A_0 + A_1 - 0.0074 * A_0 + A_2 - 0.0037 * (A_1 - 0.0074 * A_0)]$.

4.5. Calculations of the extent of labeling in the nitro group of mono-^{15}N-labeled dioxypyrrolomycin (2)

The portion (assumed x%) of the total mono-^{15}N-labeled **2** bearing a ^{15}N-labeled nitro group contributed solely to the $^{15}NO_2^{1-}$ fragment, while the remaining portion ($1 - x$%) of the mono-^{15}N-labeled **2** bearing a unlabeled nitro group contributed to the $^{14}NO_2^{1-}$ fragment ion. The ^{13}C isotopic ion of the unlabeled **2** also contributed to the $^{14}NO_2^{1-}$ fragment ion with $A_0 * 13\%$ portion, where A_0 is the measured relative abundance of the monoisotopic peak (unlabeled) and 13% is the calculated abundance ratio between the naturally occurring ^{13}C and the monoisotopic peaks of unlabeled **2**. The measured $^{15}NO_2^{1-}/^{14}NO_2^{1-}$ abundance ratio should equal to $A_1 * x\%/(A_1 - A_1 * x\% + A_0 * 13\%)$, where A_1 is the measured relative abundance of the mono-^{15}N-labeled peaks. The solutions for x can be easily found (e.g., $x = 77$ and 85 for cases **B** and **C**, respectively).

4.6. FTMS/MS on the isolated m/z 383 peak of the ^{15}N-labeled dioxapyrrolomycin (2)

FTMS SORI-CID mass spectra on the isolated m/z 383 ion were also acquired as shown in Figure 5A2–D2 for cases **A–D,** respectively, to provide additional supporting evidences for the assignments of the portions of mono-^{15}N-labeled **2** bearing a ^{15}N-labeled nitro group derived from the FTMS/MS of the mono-^{15}N-labeled ion at m/z 382. Pronounced isotopic patterns with the dominant $^{14}NO_2^{1-}$ ion over the much less abundant $^{15}NO_2^{1-}$ ion were detected for cases **A** and **B** (Fig. 5A2 and B2, Supplementary Materials Table S3). Such a result was much anticipated given that the m/z 383 precursor ion for cases **A** and **B** represented mainly the ^{37}Cl isotope of the unlabeled **2** where all nitrogen atoms are not labeled. The increased abundance of the $^{15}NO_2^{1-}$ fragment ion with ~24% relative to $^{14}NO_2^{1-}$ (100%) in case **B** resulted from the contribution of the ^{13}C isotopic ion of the mono-^{15}N-labeled **2**, which has a high portion (77%) of ^{15}N-labeled nitro group.

Different $^{15}NO_2^{1-}/^{14}NO_2^{1-}$ isotopic pattern (Fig. 5C2, Supplementary Materials Table S3) was detected for the m/z 383 precursor ion (containing $^{15}N_2$, ^{37}Cl, and $^{15}N^{13}$C isobars, see Fig. 5C) in case **C**, reflecting the collective contributions from the three major

isobars. The dominant $^{15}N_2$ isobar yielded the $^{15}NO_2{}^{1-}$ only, while the $^{15}N^{13}C$ isobar yielded mainly the $^{15}NO_2{}^{1-}$ with some portion of $^{14}NO_2{}^{1-}$. The ^{37}Cl isotopic ion from the unlabeled **2,** where all nitrogen atoms are not labeled, yielded only the $^{14}NO_2{}^{1-}$ fragment ion. A dominant $^{15}NO_2{}^{1-}$ peak was detected in case **D,** reflecting the major contribution from the abundant $^{15}N_2$-labeled **2** (Fig. 5D2, Supplementary Materials Table S3), where both nitrogen atoms were ^{15}N-labeled.

4.7. Fermentation

^{15}N- and D-labeled diazepinomicin: 0.5 mg/mL each of $^{15}N_2$-L-tryptophan, D_4-L-tyrosine (phenyl-D_4) and L-tryptophan (indole-D_5) were added into freshly prepared production medium (Bennett's, 10 mL ea, pH ~ 7.3). Labels were dissolved in Bennett's medium by applying heat (water bath at 50 °C) and sonication. Following addition of the labels, the pH of the media was re-adjusted to ~7.3 by adding dilute NaOH, filter sterilized and transferred into culture flasks (50 ml Erlenmeyer). To each of the flasks were added 5% sterilized HP-20 resin beads and 2% inoculum (seed solution of the diazepinomicin producing organism DPJ15). Flasks were incubated at 28 °C and 200 rpm and harvested after 4 days. The resin-bound ^{15}N- and D-labeled diazepinomicin analogues were extracted into MeOH, concentrated to dryness and the crude residue was purified by HPLC (Phenomenex Luna 5 μm C18, 250 × 10 mm; aqueous acetonitrile solvent gradient).

^{15}N-labeled dioxapyrrolomycin: Dioxapyrrolomycin producing culture (LL-F42248) was grown according to the general fermentation conditions described previously.[16] Under each of the growth conditions (**A**–**D**), the standard production medium was modified by omitting L-proline and $NaNO_3$ and adding 1.0 gL^{-1} of L-[^{15}N]-proline and L-[^{14}N]-arginine (case **A**), L-[$^{15}N_2$]-guanidino arginine and L-[^{14}N]-proline (case **B**), L-[$U^{15}N_4$]-arginine and L-[^{14}N]-proline (case **C**) and L-[^{15}N]-proline (case **D**). Fermentations were incubated at 28 °C and 200 rpm and harvested after 3 days. The resin-bound pyrrolomycins were extracted into acetone, concentrated to dryness and the crude residue was purified by HPLC (Phenomenex Luna 5 μm C18, 250 × 10 mm; aqueous acetonitrile solvent gradient) to obtain ^{15}N-labebed dioxapyrrolomycin.

Acknowledgments

The authors sincerely appreciate the help provided by Dr. Marshall M. Siegel in critically reviewing the manuscript and providing valuable suggestions.

Supplementary data

Supplementary data associated with this article can be found, in the online version, at doi:10.1016/j.bmc.2008.10.073.

References and notes

1. Koehn, F. E.; Carter, G. T. *Nat. Rev. Drug Disc.* **2005**, *4*, 206.
2. Newman, D. J.; Cragg, G. M.; Snader, K. M. *J. Nat. Prod.* **2003**, *66*, 1022.
3. Singh, S. B.; Barrett, J. F. *Biochem. Pharmacol.* **2006**, *71*, 1006.
4. Simmons, T. L.; Coates, R. C.; Clark, B. R.; Engene, N.; Gonzalez, D.; Esquenazi, E.; Dorrestein, P.; Gerwick, W. H. *Proc. Natl. Acad. Sci. U.S.A.* **2008**, *105*, 4587.
5. Khosla, C.; Keasling, J. D. *Nat. Rev. Drug Disc.* **2003**, *2*, 1019.
6. Marshall, A. G.; Hendrickson, C. L.; Jackson, G. S. *Mass Spectrom. Rev.* **1998**, *17*, 1.
7. Feng, X.; Siegel, M. M. *Anal. Bioanal. Chem.* **2007**, *389*, 1341.
8. Huang, J.; Tiedemann, P. W.; Land, D. P.; McIver, R. T.; Hemminger, J. C. *Int. J. Mass Spectrom. Ion Processes* **1994**, *134*, 11.
9. Shi, S. D.-H.; Hendrickson, C. L.; Marshall, A. G. *Proc. Natl. Acad. Sci. U.S.A.* **1998**, *95*, 11532.
10. Guan, S.; Marshall, A. G.; Scheppele, S. E. *Anal. Chem.* **1996**, *68*, 46.
11. Gauthier, J. W.; Trautman, T. R.; Jacobson, D. B. *Anal. Chim. Acta* **1991**, *246*, 211.
12. Little, D. P.; Speir, J. P.; Senko, M. W.; O'Cornnor, P. B.; McLafferty, F. W. *Anal. Chem.* **1994**, *66*, 2809.
13. Charan, R. D.; Schlingmann, G.; Janso, J.; Bernan, V. S.; Feng, X.; Carter, G. T. *J. Nat. Prod.* **2004**, *67*, 1431.
14. Bachmann, B. O.; McAlpine, J. B.; Zazopoulos, E.; Farnet, C. M.; Piraee, M. WO 2004/065591 A1, 2004.
15. Carter, G. T.; Nietsche, J. A.; Goodman, J. J.; Torrey, M. J.; Dunne, T. S.; Borders, D. B.; Testa, R. T. *J. Antibiot.* **1987**, *40*, 233.
16. Charan, R. D.; Schlingmann, G.; Janso, J.; Bernan, V. S.; Feng, X.; Carter, G. T. *J. Nat. Prod.* **2005**, *68*, 277.
17. Carter, G. T.; Nietsche, J. A.; Goodman, J. J.; Torrey, M. J.; Dunne, T. S.; Siegel, M. M.; Borders, D. B. *J. Chem. Soc., Chem. Commun.* **1989**, *40*, 1271.
18. Charan, R. D.; Schlingmann, G.; Bernan, V. S.; Feng, X.; Carter, G. T. *J. Nat. Prod.* **2006**, *69*, 29.
19. Kers, J. A.; Wach, M. J.; Krasnoff, S. B.; Widom, J.; Cameron, K. D.; Bukhalid, R. A.; Gibson, D. M.; Crane, B. R.; Loria, R. *Nature* **2004**, *429*, 79.
20. Zhang, X.; Parry, R. J. *Antimicrob. Agents Chemother.* **2007**, *51*, 946.
21. McAlpine, J. B.; Banskota, A. H.; Charan, R. D.; Schlingmann, G.; Zazopoulos, E.; Piraee, M.; Janso, J.; Bernan, V. S.; Aouidate, M.; Farnet, C. M.; Feng, X.; Zhao, Z.; Carter, G. T. *J. Nat. Prod.* **2008**, *71*, 1585.
22. Palmblad, M.; Hakansson, K.; Hakansson, P.; Feng, X.; Cooper, H. J.; Giannakopulos, A. E.; Derrick, P. J. *Eur. J. Mass Spectrom.* **2000**, *6*, 267.